

# Ultra-High Brightness Quantum-Dot Light-Emitting Diodes with ZnO Nanoparticles Charge-Control Layer

Chih-Jung Chen<sup>a</sup>, You-Huei Jhang<sup>b</sup>, Chung-Kai Chi<sup>b</sup>, Hsin-Chieh Yu<sup>b\*</sup>,  
and Ray-Kuang Chiang<sup>a,\*</sup>

<sup>a</sup>Taiwan Nanocrystals Corp., Ltd., Tainan, Taiwan, R.O.C.

<sup>b</sup>Institute of Lighting and Energy Photonics, College of Photonics,  
National Yang Ming Chiao Tung University, Tainan 711, Taiwan, R.O.C.

\* [rkc.chem@msa.hinet.net](mailto:rkc.chem@msa.hinet.net) and [hcYu@nycu.edu.tw](mailto:hcYu@nycu.edu.tw)

## Abstract

*This study explores the performance enhancement of QLEDs by incorporating ZnO nanoparticles (ZnO NPs) as a charge control layer (CCL) between two quantum dot emitting layers. The utilization of the CCL significantly improves the device's luminance performance, achieving a maximum luminance ( $L_{max}$ ) of 102,029 cd/m<sup>2</sup> for blue, 2,191,507 cd/m<sup>2</sup> for green, and 870,199 cd/m<sup>2</sup> for red. This demonstration creates a new route to design impact QLED architecture for next generation displays and lighting.*

## Author Keywords

Quantum dots, light-emitting diode, ultra-high brightness, ZnO, nanoparticle

## 1. Introduction

Quantum dots (QDs) are exceptional optoelectronic materials for photoluminescence (PL) and electroluminescence (EL) applications, owing to their unique properties, such as narrow emission bandwidths, high brightness, size-tunable emission wavelengths, and broad absorption spectra. [1] Electrically pumped quantum dot light-emitting diodes (QLEDs) have shown promise in display and lighting technologies, with continuous improvements in efficiency, brightness, and long-term stability. For effective lighting applications, the brightness threshold must exceed 10<sup>3</sup> to 10<sup>4</sup> nits. However, most current QLED devices have focused primarily on indoor displays, achieving high efficiency but relatively low luminance. Therefore, a significant challenge remains in achieving both high luminance and high efficiency across the three primary colors in EL devices—essential for applications in outdoor displays, microdisplays, projectors, and lighting. [2]

Over the past decade, there has been a significant shift in the design of core-shell quantum dot (QD) nanostructures, from thin shells to thicker shells. This evolution has enabled QDs to exhibit unique properties, including reduced single-dot photoluminescence (PL) blinking, lower nonradiative Auger recombination rates, increased stability, a larger Stokes shift, and improved electroluminescence (EL) performance. As a result, QLEDs using thick-shell QDs in their emission layers can achieve higher brightness under intense current driving conditions, thanks to their excellent thermal stability, minimized Auger effects, and reduced energy transfer losses between QDs. [3] In our research, we developed thick-shell QDs with core-shell-shell structures: CdSe/CdZnSe/ZnS for blue QLEDs, CdSe/CdZnSe/ZnS for green QLEDs, and CdSe/CdZnSe/CdZnS for red QLEDs.

In QLEDs, radiative emission of excitons in quantum dots is typically achieved through the direct injection of charge carriers or energy transfer from the surrounding matrix or adjacent charge transport layers with higher energy levels. Controlling carrier injection with a balanced rate from both electron and hole sides ensures that electron-hole pairs recombine radiatively within the emission layer, significantly enhancing QLED performance. For instance, some studies have proposed the incorporation of an additional charge control layer (CCL) within the emission layer to improve performance. [4-6] In previous work, we used an ultra-thin poly(N-vinylcarbazole) (PVK) CCL, which enhanced charge balance, reduced carrier leakage, and optimized energy levels within the device, thus improving its optoelectronic performance. [4] In this study, we employed inorganic ZnO nanoparticles as the CCL, placed between two QD emission layers to manipulate the balance of injected carriers. The ZnO NPs prevent intermixing of the emission layers, offer good solution processability, and align well with the device's energy levels. Additionally, ZnO provides strong environmental stability and high electron mobility, further boosting the device's efficiency. Incorporating the ZnO CCL significantly enhances the luminance performance, achieving maximum luminance ( $L_{max}$ ) values of 102,029 cd/m<sup>2</sup> for blue, 2,191,507 cd/m<sup>2</sup> for green, and 870,199 cd/m<sup>2</sup> for red. This work lays the groundwork for innovative QLED architectures for next-generation displays.

## 2. Results and Discussion

### 2.1 Preparation of Thick-Shell QDs

Thick-shell core-shell quantum dots (QDs) with CdSe/CdS and CdSe/ZnSe compositions were developed initially, exhibiting unique properties such as low non-radiative Auger recombination, reduced single-dot photoluminescence (PL) blinking, enhanced stability, and a large Stokes shift. [7] These characteristics make them highly valuable for improving electroluminescence in quantum dot light-emitting diodes (QLEDs). However, despite these advantages, thick-shell QDs with such compositions typically exhibit moderate photoluminescence quantum yields (PLQY) due to lattice strain accumulated during the growth of the thick shell. In contrast, QDs with composition-gradient shells experience less lattice mismatch and therefore accumulate little strain as the shell thickness increases. Furthermore, the band gap alignment in these gradient shells can be gradually adjusted, which benefits carrier injection during the electroluminescent (EL) process. This can be achieved by selecting an appropriate composition ratio among the elements cadmium (Cd), zinc (Zn), selenium (Se), and sulfur (S) in II-VI group semiconductors. Gradient

shells can be effectively fabricated using techniques such as alloying and cation or anion exchange of II-VI compounds, as the band gap and lattice constant vary in the sequence CdSe, CdS, ZnSe, and ZnS. In this study, we prepared thick-shell QDs with core-shell-shell structures: CdSe/CdZnSe/ZnS for blue-emitting QDs, CdSe/CdZnSe/ZnS for green-emitting QDs, and CdSe/CdZnSe/CdZnS for red-emitting QDs. Figure 1 presents TEM micrographs of the resulting thick-shell QDs. The diameters of the QDs are approximately 9 nm, 12 nm, and 15 nm for blue, green, and red-emitting QDs, respectively. The emission characteristics of the QDs are as follows: blue QDs emit at 468 nm (FWHM = 24 nm, QY = 90%), green QDs emit at 530 nm (FWHM = 28 nm, QY = 95%), and red QDs emit at 626 nm (FWHM = 24 nm, QY = 98%).

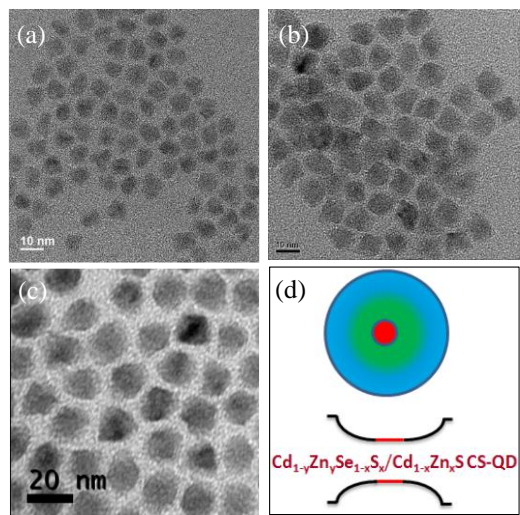


Figure 1. The TEM micrographs of (a) blue, (b) green, and (c) red QDs. (d) schematic diagram of the thick-shell QDs.

### 2.2 Device fabrication and performance

Figure 2 shows schematic illustration of green QLEDs structure and energy band diagram. [3] The thickness of each layer is presented in the parentheses. The optimal thickness of ZnO CCL is determined to be around 15 nm which thickness is smaller than typical ZnO or Zn<sub>x</sub>Mg<sub>1-x</sub>O NP electron transport layer (ETL) of 50 nm to 100 nm. This ultra-thin ZnO CCL possessed the capability of increasing the radiative recombination of excitons by reducing the predominant electrons, adjusting the charge injection rate, and thus suppressing QD charging effect.

Figure 3(a) presents the EL spectra of the green QLEDs with single layer and bilayers, respectively. The emission wavelength of two devices is 538 nm, and the FWHM is about 29 nm. Conventional QLEDs without ZnO CCL was labeled as single layer (QLED-A), and the device with ZnO CCL was labeled as bilayers (QLED-B). The completely overlapping EL spectra showed no energy transferred between QD layers after integration of ZnO CCL. Fig. 3(b) presents the operating current density of these two green QLEDs. The inclusion of the CCL did not reduce the operating current density of the devices; in fact, the turn-on voltage of about 2.2 V was even lower than that of 2.4 V of QLED-A at a luminance of 10 cd/m<sup>2</sup>, as depicted in the inset of Fig. 3(b). Fig. 3(c) reveals that the  $L_{max}$  of the QLED-B with CCL reached up to 2,191,507 cd/m<sup>2</sup> at 6.8 V, significantly brighter than the QLED-A without CCL, with QLED-B's brightness nearly 342% higher than QLED-A's

brightness of 495,721 cd/m<sup>2</sup> at 5.6 V. Fig. 3(d) shows that the maximum current efficiency (CE) of the green QLEDs with ZnO CCL was approximately 49.1 cd/A, which is 173% higher than the  $CE_{max}$  of QLED-A, which was 18.1 cd/A.

Similarly, we also fabricated blue and red QLED devices with and without ZnO NP CCL. Figure 4(a) and 4 (b) showed no significant difference in emission wavelength and FWHM after integrating ZnO CCL. The emission wavelength and FWHM are 472 nm and 27 nm for blue devices, and 634 nm and 27 nm for red devices. Figure 4(c) and Figure 4(e) revealed that the  $L_{max}$  and the CE of the blue QLEDs are 102,029 cd/m<sup>2</sup> and 3.1 Cd/A, that showed 65% and 59% improvements, respectively, compared to single layer device. Figure 4(d) and Figure 4(f) revealed that the  $L_{max}$  and the CE of the red QLEDs are 870,199 cd/m<sup>2</sup> and 15.9 Cd/A, that showed 111% and 60% improvements, respectively, compared to single layer device.

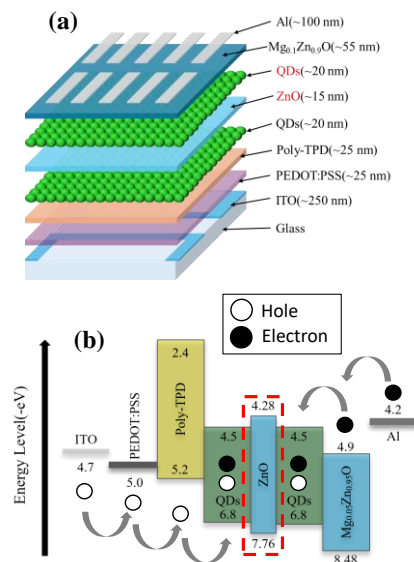


Figure 2. Schematic illustration of (a) green QLEDs structure and (b) energy band diagram

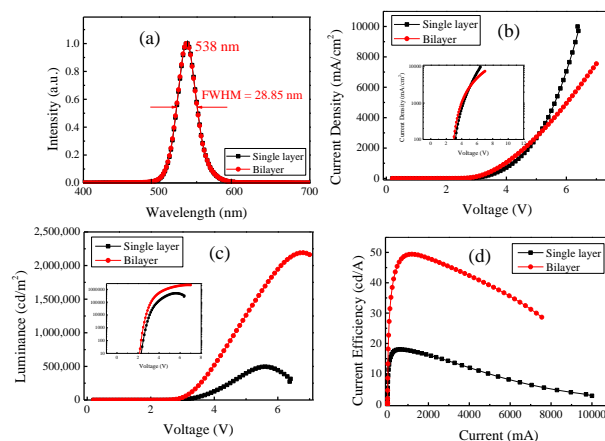
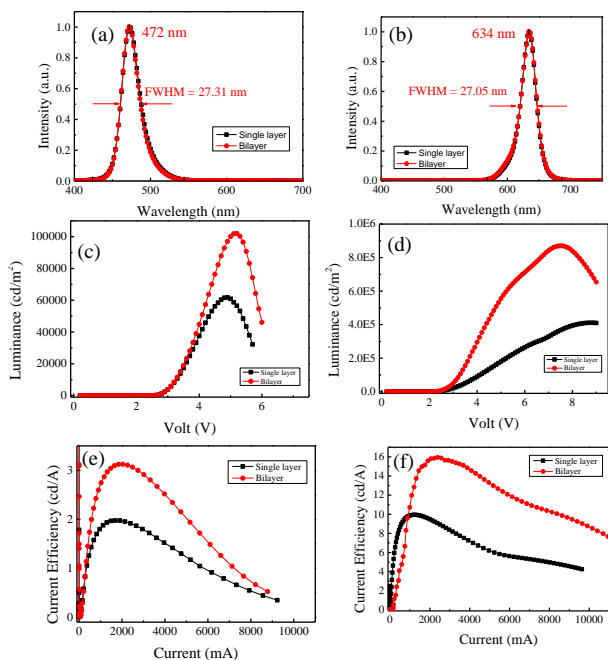


Figure 3 (a) Emission spectra, (b) J-V curves, (c) L-V curves and (d) current efficiency to current density (CE-J) relationships of green QLEDs with and without ZnO NPs CCL, single layer devices (black square) and the bilayer devices (red circle).



**Figure 4** (a, b) Emission spectra, (c,d) L-V curves and (e,f) current efficiency to current density (CE-J) relationships of blue and red QLEDs with and without ZnO NPs CCL, single layer devices (black square) and the bilayer devices (red circle).

**2.3 Mechanisms for the high device performance**

To investigate the impact of ZnO CCL on electron injection, we fabricated electron-only devices (EOD) and hole-only devices (HOD) for both green QLED-A and QLED-B to analyze the current-to-voltage (I-V) curves, as illustrated in Figure 5. The EOD structures for QLED-A and QLED-B are composed of Al/ZnMgO/QDs and Al/ZnMgO/QDs/ZnO/QDs, respectively. Meanwhile, the HOD structures for both devices consist of QD/poly-TPD/PEDOT:PSS/ITO. The results indicated that the I-V curves for the EOD and HOD using QLED-B are more coincident compared to those of QLED-A, as shown in Figure 5. In devices without the ZnO CCL, the injected electrons tend to overflow into the poly-TPD layer, which results in lower overall efficiency. In contrast, introducing a ZnO CCL can regulate electron transport, which enhance carrier balance injection and leads to more efficient radiative recombination. Furthermore, using two quantum dot (QD) emissive layers provides better electron confinement, resulting in higher recombination efficiency. Additionally, the improvement in I-V curve alignment occurs within an applied voltage range of 0 V to 3.5 V. This suggests that carrier injection becomes more balanced at lower applied voltages, causing the turn-on voltage to decrease from 2.4 V (without CCL) to 2.2 V (with CCL), as illustrated in Figure 3(c).

**2.4 Device lifetime**

The lifetime of the two green QLED devices is evaluated by measuring the luminance over time at constant current densities, as shown in Figure 6. The results are fitted by an empirical equation,  $L_0^n T_{50} = \text{constant}$  where  $L_0$ ,  $n$  and  $T_{50}$  are the initial brightness, acceleration factor and half lifetime, respectively.  $n$  is determined to be 1.96 for the two devices. These findings

indicate that the lifetime  $T_{50}$  at 100 nits for the bilayer device is 131,955 hours, which represents a 489% improvement compared to the single-layer device with a  $T_{50}$  at 100 nits of 22,381 hours. The excellent stability of the bilayer device, combined with its high luminance output, low efficiency roll-off, and low turn-on voltage, positions QLEDs as promising candidates for the next generation of flat panel displays and lighting systems.

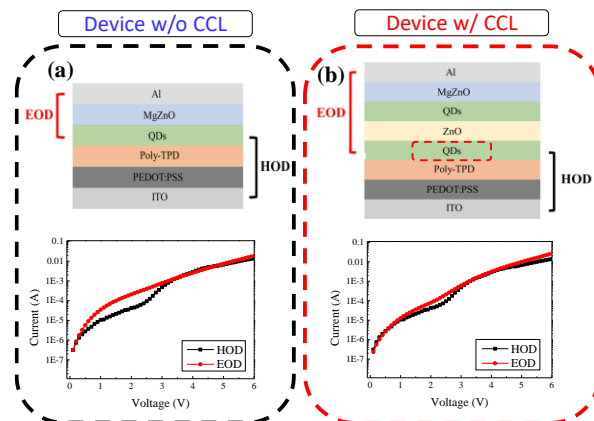


**Figure 5.** I-V curve for electron-only devices (EOD) and hole-only devices (HOD) in (a) QLED-A and (b) QLED-B devices.

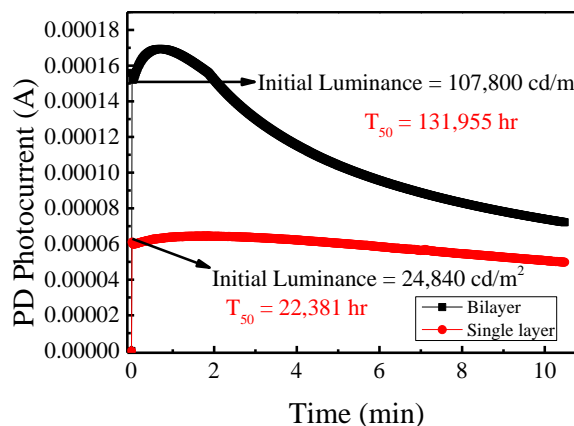


**Figure 6.** The luminance output vs. operation time of green QLEDs with bilayer and single layer structures.

**3. Summary**

This study proposes a novel structure for QLEDs by incorporating ultra-thin zinc oxide nanoparticles as a charge control layer between the quantum dot emitting layers. This design can help to regulate electron transport, resulting in a balanced carrier injection. Consequently, the device demonstrates excellent stability, high luminance output, low efficiency roll-off, and a low turn-on voltage. These features position QLEDs as promising candidates for next-generation display and lighting systems.

## Experimentals

**Preparation of ZnO NPs.** ZnO and Mg<sub>0.1</sub>Zn<sub>0.9</sub>O NPs is prepared by a low-temperature solution synthesis method based on previously reported method [8]. 0.59 g zinc acetate dehydrate and 0.2569 g magnesium nitrate hexahydrate is dissolved in 25 mL of methanol and heated in water-bath at 60 °C. Then, 13 mL of KOH solution (4.6 mmol dissolved in methanol) is added dropwise into the zinc acetate solution at 60–65 °C. After stirring for 2.5 h, the solution is subjected to centrifuge at 6000 rpm for 10 min and the colloidal precipitation is thoroughly washed with methanol once. Finally, the precipitation is redispersed in a mixture of 12 mL n-butanol and 1 mL chloroform[9].

**Fabrication of QLEDs.** After cleaning the ITO-coated glass substrates with detergent and DI water, followed by acetone and isopropyl alcohol, the ITO glass was subjected to UV-ozone treatment for 25 minutes to facilitate surface modification and improve wettability. Subsequently, PEDOT: PSS thin film was spin-coated at 4000 rpm for 40 seconds and baked at 120°C for 15 minutes. Poly-TPD was dissolved in chlorobenzene with a concentration of 8 mg/mL, spin-coated at 4000 rpm for 40 seconds, and baked at 110°C for 30 minutes in a nitrogen-filled glove box to form the HTL. The quantum dots were spin-coated at 2000 rpm for 35 seconds and baked at 80°C for 30 minutes in the glove box. Subsequently, ZnO NPs and MZO NPs, synthesized by the low-temperature solution method as previously reported [9], were used as the CCL and ETL, respectively. The CCL was spin-coated at 7000 rpm for 20 seconds, and the ETL at 3000 rpm, with both layers baked at 80°C for 30 minutes each. Finally, a 100 nm-thick aluminum layer was thermally evaporated onto ETL to serve as the cathode and the QLEDs fabrication process is completed.

## Instrumentation

PL spectra and PLQY were obtained on a fluorescence spectrophotometer (FluoroMax-Plus, HORIBA JOBIN YVON). The electroluminescence properties including emission spectra and luminance of the fabricated devices are measured by using Photo Research PR-670 Spectra Scan Colorimeter. Keysight

B2912B source-meter is used to drive the QLEDs and record the current-voltage (I–V) curves. The fabricated QLEDs are not packaged or hermetically sealed and all measurements are carried out in the nitrogen-filled glove box to avoid the influence of oxygen and moisture on QLEDs performance.

## Acknowledgment

The authors would like to thank the financial support from National Science and Technology Council of Taiwan, Republic of China, under contract No. NSTC 112-2221-E-A49-133-MY3.

## Reference

- [1] Jang, H.J., Lee, J.Y., Baek, G.W., Kwak, J., and Park, J.H., *J. Inf. Display* 23, 1-17 (2022)
- [2] Shen, H., Gao, Q., Zhang, Y., Lin, Y., Lin, Q., Li, Z., Chen, L., Zeng, Z., Li, X., Jia, Y., Wang, S., Du, Z., Li, L.S. and Zhang, Z. *Nature Photonics* 12, 192-197 (2019)
- [3] Chen, C.J., Lien, J.Y., Wang, S.L., Chiang, R.K., *J. Soc. Inf. Display*. 39-1 (2017)
- [4] Vu, H.T., Huang, C.Y., Yu, H.C., Su, Y. K., *Org. Electron.*, 63, 349–354 (2018)
- [5] Wang, L., Pan, J., Qian, J., Lei, W., Wu, Y., Zhang, W., Goto, D.K., Chen, J., *J. Mater. Chem. C* 6(30), 8099–8104 (2018)
- [6] Lee, K.H., Han, C.Y., Jang, E.P., Jo, J.H, Hong, S., Hwang, J.Y., Choi, W., Hwang, J.H., Yang, H., *Nanoscale* 10(14), 6300–6305, 2018
- [7] Pal, B.N., Ghosh, Y., Brovelli, S., Laocharoensuk, Klimov, V.I., Hollingsworth, J.A. and Htoon, H., *Nano Lett.* 12, 331–336 (2012)
- [8] Zhu, Y., Hu, H., Liu, Y., Chen, M., Lin, W. Ye, Y., Guo, T., Li, F., *Organic Electronics* 70, 279-285 (2019)
- [9] Y. H.C., Zhuo, Q.H., Shi, J.T., Chu, K.H., *Organic Electronics* 110,106646 (2022)